

## EXAMINATION OF GRAPHENE WITH VERY SLOW ELECTRONS

Eliška MIKMEKOVÁ, Luděk FRANK

*Institute of Scientific Instruments of the ASCR, v. v. i., Královopolská 147, 61264 Brno, ludek@isibrno.cz*

### Abstract

Although graphene has been available and intensively studied for nearly a full decade, new methods are still required for its examination and diagnostics. Even checking the continuity of layers and the reliable counting of layers of graphene and other 2D crystals should be easier to perform. Scanning electron microscopy with slow and very slow electrons offers an innovative tool enabling one to see graphene samples at nanometer or even sub-nanometer lateral resolution in both transmitted and reflected electrons and to count the number of layers reliably in both imaging modes. Diagnostics can be performed in this way on freestanding graphene samples as well as on graphene grown on the surfaces of bulk substrates. Moreover, bombardment with very slow electrons acts as an ultimate cleaning procedure removing adsorbed gases from crystal surfaces which can be monitored in scanned transmission electron images taken at below 50 eV.

### Key words:

Graphene, slow electrons, very low energy scanning electron microscopy, ultralow energy STEM

### 1. INTRODUCTION

Interest in graphene has been growing in recent years since the mechanical exfoliation method was first described [1]. The interesting properties of graphene, including its conductivity and transparency, make it extremely attractive for many applications.

Basically, we can divide the preparation methods for graphene into two groups: exfoliation (stripping from already existing graphite crystal) and the direct growth of graphene on various substrates by means of Chemical Vapor Deposition (CVD), epitaxial growth, etc. The liquid phase exfoliation procedure dispersing graphite in an organic solvent [2] can prepare graphene of high quality and purity, but the size of the flakes is extremely small. Direct growth on substrates offers better prospects for making graphene in useable sizes [3,4]. Graphene samples have been examined by conventional TEM and STEM methods at high energies that are capable of visualizing single atoms and, therefore, structure defects as well [5-7]. An SEM equipped with a cathode lens that enables one to reduce the electron beam energy to tens or units of eV at an acceptable resolution of the image [8] offers an additional tool for examining graphene in a non-traditional transmission as well as reflection mode.

The scattering of incident electrons in solid targets can be described as collisions with atomic cores. When decreasing energy to units of keV, the scattered electrons see the cores surrounded with atomic jellium and interact more and more with the target electrons. In the range of hundreds of eV, the electron-electron interaction intensifies and also includes correlation and exchange phenomena [9]. Generally, the scattering rate of electrons in solids increases with the decreasing energy of their impact so that image contrasts in microscopes are steeply enhanced. Below 20 or 30 eV, we meet the band structure range, the incident electrons transform into Bloch waves within a dispersion relation corresponding to the crystal system and its spatial orientation, and scatter as these waves [10]. Thus, slow electrons probe just the electronic structure of the target. From the point of view of scattering statistics, the inelastic scattering of electrons in solids achieves its highest rate, i.e. shortest mean free path (IMFP), at around 50 eV for virtually all materials [11]. Below this minimum, the IMFP starts extending again. The elastic mean free path (EMFP) shortens continuously with the decreasing energy of electrons even below 50 eV, so in this range the penetration of incident electrons, governed by the total "transport" mean free path, remains questionable. However, it may

be expected to extend in crystalline targets providing directions of a high density of empty electron states. In this respect, very low energy microscopy in the scanning transmission mode has promising prospects for the examination of graphene.

Raman spectroscopy represents an acknowledged method of diagnostics for graphene sheets. The structure of the phonon dispersion of graphene [12] leads to a Raman spectrum with two simple dominant features, namely the G-band ( $\sim 1,580 \text{ cm}^{-1}$ ) and the G'-band ( $\sim 2,700 \text{ cm}^{-1}$ ). The height ratio of G-peak to G'-peak is well below 1 for graphene, but exceeds 1 for graphite. The G'-band of multilayer graphene is moved to a higher Raman shift with respect to its original position of  $2,687 \text{ cm}^{-1}$  and becomes broader than that for single-layer graphene. The G'-band can be fit with just a single sharp and symmetric peak of a Lorentzian shape only for single-layer graphene. When the number of graphene layers increases, the relative intensity of the G'-band decreases and other components appear, leading to the up-shift of the band. In this way, it is possible to differentiate a single layer from a bi-layer and from multiple-layer sites. However, diagnostics of graphene based on Raman spectroscopy is limited by its lateral resolution to hundreds of nm, i.e. two to three orders of magnitude worse than that of S(T)EM or TEM.

## 2. LOW ENERGY ELECTRON MICROSCOPY OF GRAPHENE

### 2.1 Specimens of graphene

Pilot experiments have been performed on two kinds of graphene samples, namely one commercially available sample prepared by the CVD method (CVD graphene<sup>TM</sup>, see [www.graphene-supermarket.com](http://www.graphene-supermarket.com)) and one liquid phase exfoliated sample provided by A. Geim and K. Novoselov. Observation of these samples, the results of which have been summarized in [13], showed the samples as consisting of small flakes, randomly overlapping each other, or even relatively thick films of a graphite nature with “windows” covered by single or multiple graphene layers combined with empty holes. Neither of the samples seemed suitable for quantitative study, i.e. collection of the necessary reference data, of slow electron transmissivity as a possible tool for counting the graphene layers.

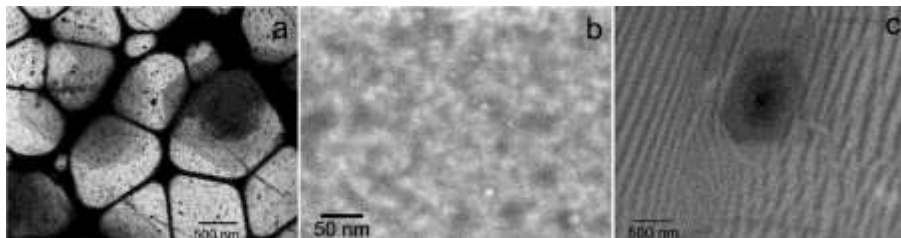


**Fig. 1** Micrographs of two graphene samples used in the study (a,b – sample A, c – sample B), standard vacuum SLEEM: transmitted electrons, 220 eV (a) and 1 keV (b), reflected signal, 200 eV (c).

This time we used two samples prepared by the CVD method. Freestanding graphene (sample A) deposited on lacey carbon was purchased (<http://www.tedpella.com/>) in three versions declared as 1LG, 2LG and 3to5LG. The lacey windows were also available in sizes of more than a micrometer with a density of nucleation centres appearing as dark dots seemingly covering only a negligible part of their area (Fig. 1a). High magnification shows the sample consisting of domains of tens or even units of nm in size (Fig. 1b). Atomic resolution microscopy was not available for this study. The second sample B was grown on polycrystalline Cu from a  $\text{CH}_4+\text{H}_2$  atmosphere at  $800 \text{ }^\circ\text{C}$ .

### 2.2 Microscopy of freestanding graphene

The freestanding graphene samples were first examined in the standard vacuum extreme high resolution SEM equipped with the cathode lens mode. Fig. 2 shows micrographs taken in the reflected electron (RE) as well as transmitted electron (TE) mode at several energies. The reflected electron signal was composed of

both secondary and backscattered electron emission, accelerated in the cathode lens field toward the detector.

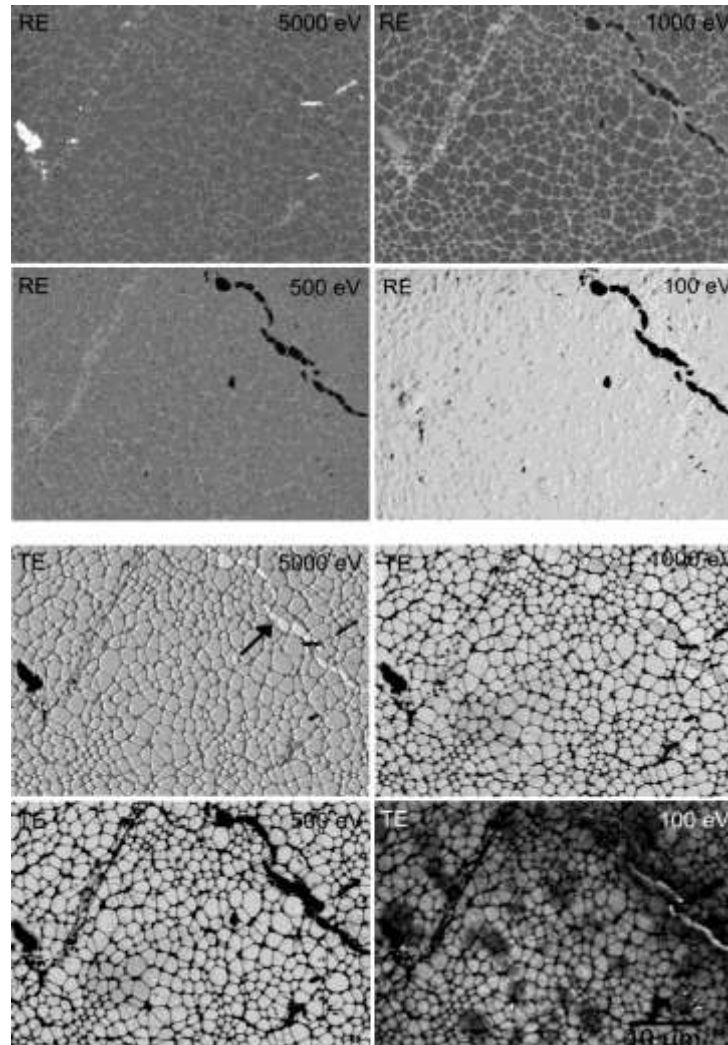


**Fig. 2** Freestanding graphene sample with islands of 3 to 5 layers.

In the RE frames the maximum contrast between the graphene layers and lacey carbon appears at 1 keV and decreases toward higher and lower energies because of extending and shortening information depth, respectively. These images identify empty holes but do not reveal thicker islands of graphene. In the TE mode we do not see multilayer graphene islands above 100 eV – this fact underlines the suitability of very low energy electron microscopy for examination of 2D crystals. Interpretation challenges are presented by some details inverting their contrast more than once (see the arrow) – these probably arise from contaminations that become charged.

### 2.3 Graphene grown on a substrate

In Fig. 3 we see a series of micrographs, again taken in the standard vacuum microscope on a Cu surface partly covered by graphene islands of various thicknesses. When decreasing the landing energy of electrons in the SEM, we steeply increase the surface sensitivity of imaging. Several authors declare the process of graphene growth on Cu as an epitaxy producing islands of single-layer graphene (e.g. Ref. [14]). To observe these islands we have to go to 500 eV (Fig. 3), but at 100 eV and below, at extreme surface sensitivity, we again stop observing the “wedding cake” of stacked layers but see its outer contour. This indicates the underlayer mechanism of nucleation and growth below already existing islands [15].

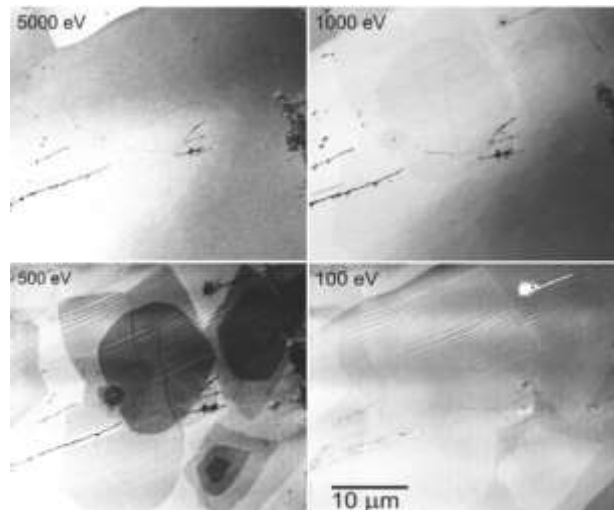


**Fig. 3** Graphene grown on polycrystalline copper.

#### 2.4 Radiation damage of contaminants

In the course of acquiring low energy micrographs in the transmission mode we noticed a gradual change in the brightness of successive scans, namely an increase in the sample transmissivity. In Fig. 4 we see a clear increase in transmissivity and decrease in reflectivity of two fields of view after prolonged observation. Fig. 5 shows changes in transmissivity due to a  $1.4 \text{ Ccm}^{-2}$  dose of electrons at various energies.

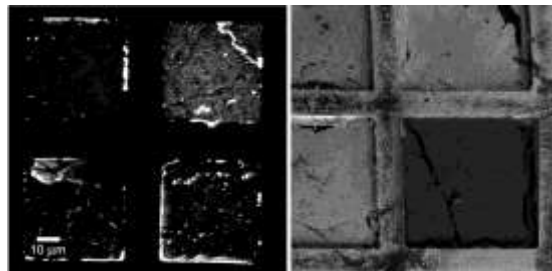


**Fig. 4** Changes in properties of 1LG due to prolonged bombardment with 30 eV electrons.

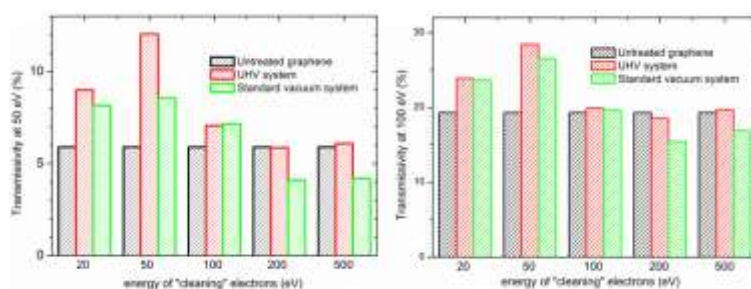


**Fig. 5** Quantitative development of 1LG transmissivity in dependence on vacuum conditions and electron energy.

The observed phenomena, i.e. a decrease in transmissivity and increase in reflectivity of graphene bombarded with very slow electrons below about 100 eV (irrespectively of the vacuum conditions) and the opposite effect taking place solely under standard vacuum conditions (but not in UHV) can be explained on the basis of the usual presence of hydrocarbon molecules adsorbed on surfaces. In a standard vacuum they are present at high density and even diffuse from the surroundings to the viewfield where they are decomposed by incident electrons and create a carbonaceous contamination layer, most intensively for electrons around 200 eV. In the UHV they are less present and contamination, if any, is reduced. Very slow electrons release hydrocarbon molecules instead of decomposing them, so the surface becomes cleaner

even in a standard vacuum. So mere observation with very slow electrons can serve as the ultimate step in the procedure of graphene cleaning.

## 2.5 Counting graphene layers

The counting of graphene layers by means of Raman spectroscopy is faced by the issue of the low lateral resolution of light optical imaging. Very low energy SEM provides much higher resolution, so it is worth checking its selectivity for the same purpose. Fig. 6 shows that the contrast of individual graphene layers is preserved down to units of eV at gradually decreasing signal-to-noise ratio. Measurement of the transmissivity was calibrated between the zero signal on mesh rungs and the full signal in empty holes. The results are shown in Fig. 7 and in Table 1.

**Table 1** Total transmissivity measured on graphene samples for 40 eV incident electrons.

No. of graphene layers	1	2	3	4	5	6	7
Transmissivity (%)	11.9	9.0	6.5	4.9	3.5	2.6	2.0

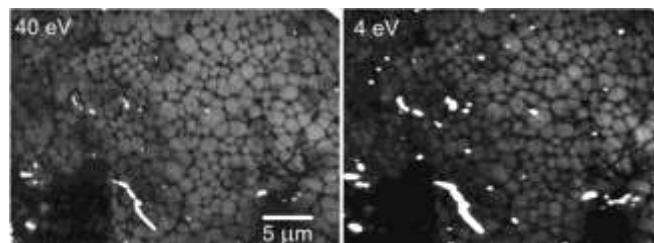


**Fig. 6** Micrographs of a 3to5LG graphene sample taken in a UHV microscope.

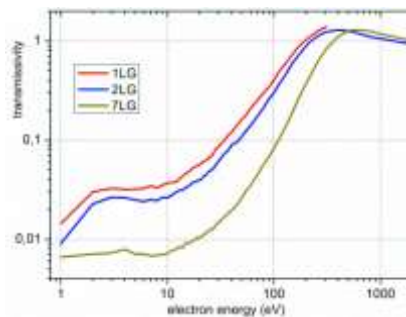


**Fig. 7** The measured energy dependence of transmissivity.

In Fig. 7 we see the graphene transmissivity exceeding 1 at hundreds of eV. This indicates an empty hole as “less transparent” than the graphene including multilayer graphene. The explanation lies in the emission of secondary electrons that are released near the bottom surface, partly emitted and accelerated in the cathode lens field toward the lower detector.



**Fig. 8** Empty hole in the graphene (see arrow) shown at 70 eV in backscattered electrons (a) and at 70 eV (b) and 600 eV (c) in transmitted electrons.

### 3. CONCLUSIONS

The scanning electron microscope operated in the low and very low energy range by means of a cathode lens is capable of providing very high contrast of samples composed of light elements sufficient to distinguish individual layers of graphene or other 2D crystals both in reflected and transmitted signals. Imaging at 30 to 50 eV enables one to count locally the graphene layers at high lateral resolution. Bombardment with electrons below 50 eV releases adsorbed hydrocarbon molecules and leaves the graphene atomically clean.

### ACKNOWLEDGEMENTS

***This study is supported by the TE01020118 project of the Technology Agency of the Czech Republic (Competence Centre: Electron Microscopy) and by MEYS CR (LO1212). Thanks are due to Mr. Jiří Sýkora for his assistance in experiments and to Mr. Baowen Liu for providing sample B.***

### LITERATURE

- [1] Novoselov, K.S., Geim, A.K., Morozov, S.V., Jiang, D., Zhang, Y., Dubonos, S.V., Grigorieva, I.V., Firsov, A.A. Electric field effect in atomically thin carbon films. *Science*, 2004, vol. 306, p. 666-669.
- [2] Lotya, M., King, P.J., Khan, U., De, S., Coleman, J.N. High-concentration, surfactant-stabilized graphene dispersions. *ACS Nano*, 2010, vol. 4, p. 3155-3162.
- [3] Cambaz, Z.G., Yushin, G., Osswald, S., Mochalin, V., Goyotsi, Y. Noncatalytic synthesis of carbon nanotubes, graphene and graphite on SiC. *Carbon*, 2008, vol. 46, p. 841-849.
- [4] Kim, K.S., Zhao, Y., Jang, H., Lee, S.Y., Kim, J.M., Kim, K.S., Ahn, J.H., Kim, P., Choi, J.Y., Hong, B.H. Large-scale pattern growth of graphene films for stretchable transparent electrodes. *Nature*, 2009, vol. 457, p. 706-710.
- [5] Meyer, J.C., Kisielowski, C., Erni, R., Rossell, M.D., Crommie, M.F., Zettl, A. Direct imaging of lattice atoms and topological defects in graphene membranes. *Nano Letters*, 2008, vol. 8, p. 3582-3586.
- [6] Huang, P.Y., Ruiz-Vargas, C.S., Van Der Zande, A.M., Whitney, W.S., Levendorf, M.P., Kevek, J.W., Garg, S., Alden, J.S., Hustedt, C.J., Zhu, Y., Park, J., McEuen, P.L., Muller, D.A. Grains and grain boundaries in single-layer graphene atomic patchwork quilts. *Nature*, 2011, vol. 469, p. 389-392.
- [7] Zhou, W., Oxley, M.P., Lupini, A.R., Krivanek, O.L., Pennycook, S.J., Idrobo, J.C. Single atom microscopy. *Microscopy and Microanalysis*, 2012, vol. 18, p. 1342-1354.
- [8] Müllerová, I., Frank, L. Scanning low energy electron microscopy. *Advances in Imaging and Electron Physics*, 2003, vol. 128, p. 309-443.
- [9] Bauer, E. Low energy electron microscopy. *Reports on Progress in Physics*, 1994, vol. 57, p. 895-938.
- [10] Bartoš, I. Electronic structure of crystals via VLEED. *Progress in Surface Science*, 1998, vol. 59, p. 197-206.
- [11] Fitting, H.-J., Schreiber, E., Kuhr, J.-C., von Czarnowski, A. Attenuation and escape depths of low-energy electron emission. *Journal of Electron Spectroscopy and Related Phenomena*, 2001, vol. 119, p. 35-47.
- [12] Malard, L.M., Pimenta, M.A., Dresselhaus, G., Dresselhaus, M.S. Raman spectroscopy in graphene. *Physics Reports*, 2009, vol. 473, p. 51-87.
- [13] Mikmeková, E., Bouyanfif, H., Lejeune, M., Müllerová, I., Hovorka, M., Unčovský, M., Frank, L. Very low energy electron microscopy of graphene flakes. *Journal of Microscopy*, 2013, vol. 251, p. 123-127.
- [14] Nie, S., Wofford, J.M., Bartelt, N.C., Dubon, O.D., McCarty, K.F. Origin of the mosaicity in graphene grown on Cu (111). *Physical Review B*, 2011, vol. 84, 155425:1-7.
- [15] Nie, S., Wu, W., Xing, S., Yu, Q., Bao, J., Pei, S., McCarty, K.F. Growth from below: bilayer graphene on copper by chemical vapour deposition. *New Journal of Physics*, 2012, vol. 14, 093028:1-9.